THE NEAR-FIELD DISTURBANCE CREATED BY A BODY IN A STRATIFIED MEDIUM WITH A FREE SURFACE

John W. Murdock

Aerospace Corporation

Prepared for:

Space and Missile Systems Organization

15 May 1975

REPORT SAMSO-TR-75-175

The Near-Field Disturbance Created by a Body in a Stratified Medium with a Free Surface

JOHN W. MURDOCK

Vehicle Engineering Division
Engineering Science Operations
The Aerospace Corporation
El Segundo, Calif. 90245

15 May 1975

Final Report

Prepared for

DEFENSE ADVANCED RESEARCH PROJECTS AGENCY
1400 Wilson Blvd.
Arlington, Va. 22209

SPACE AND MISSILE SYSTEMS ORGANIZATION
AIR FORCE SYSTEMS COMMAND
Los Angeles Air Force Station
Los Angeles, Calif. 90045

UNCLASSIFIED

SECURITY CLASSIFICATION OF THIS PAGE (When Data Entered)

REPORT DOCUMENTATION PAGE		READ INSTRUCTIONS BEFORE COMPLETING FORM
1. REPORT NUMBER SAMSO-TR-75-175	2. GOVT ACCESSION NO.	3. RECIPIENT'S CATALOG NUMBER
4. TITLE (and Subtitle) THE NEAR-FIELD DISTURBANCE CREATED BY A BODY IN A STRATIFIED MEDIUM WITH A FREE SURFACE		5. TYPE OF REPORT & PERIOD COVERED Final - Oct 1974-Feb 1975 6. PERFORMING ORG. REPORT NUMBER TR-0075(5649)-1
7. AUTHOR(s) John W. Murdock		8. CONTRACT OR GRANT NUMBER(s) F04701-74-C-0075 DARPA Order No. 2843
9. PERFORMING ORGANIZATION NAME AND ADDRESS The Aerospace Corporation El Segundo, Calif. 90245		10. PROGRAM ELEMENT, PROJECT, TASK AREA & WORK UNIT NUMBERS
11. CONTROLLING OFFICE NAME AND ADDRESS Space & Missile Systems Organization Los Angeles Air Force Station Los Angeles, Calif. 90045		12. REPORT DATE 15 May 1975 13. NUMBER OF PAGES ~~X~~ 51
14. MONITORING AGENCY NAME & ADDRESS(if different from Controlling Office) Defense Advanced Research Projects Agency 1400 Wilson Blvd. Arlington, Va. 22209		15. SECURITY CLASS. (of this report) Unclassified 15a. DECLASSIFICATION/DOWNGRADING SCHEDULE

16. DISTRIBUTION STATEMENT (of this Report)

Approved for public release; distribution unlimited.

17. DISTRIBUTION STATEMENT (of the abstract entered in Block 20, if different from Report)

18. SUPPLEMENTARY NOTES

19. KEY WORDS (Continue on reverse side if necessary and identify by block number)

Stratified flow

Internal waves

20. ABSTRACT (Continue on reverse side if necessary and identify by block number)

The inviscid equations of motion for a slender body in a stratified fluid are formulated in a way which clearly illustrates the relation between the vorticity in the flow and the internal wave behavior. This formulation makes it clear that the problem admits a singular perturbation expansion of the solution if the density variation is small (large Vaisala length). Analytic solutions valid in the near field are obtained for the case of a finite-thickness constant thermocline. These solutions include both internal wave

DD FORM 1473 (FACSIMILE)

UNCLASSIFIED

SECURITY CLASSIFICATION OF THIS PAGE (When Data Entered)

19. KEY WORDS (Continued)

20. ABSTRACT (Continued)

and gravity wave perturbations to the basic potential flow. The slender body approximation is found to be invalid near the body; the use of this approximation results in a singularity behind the body which extends to infinity. The reason for the appearance of the singularity is given, and a technique for eliminating it is outlined. The effect of the singularity on the solution at the surface is found to be small. Typical behavior of the near-field surface current is presented in graphical form. The near-field surface disturbance is found to result primarily from the basic body potential flow field with significant corrections made as a result of the stratification.

PREFACE

The author is pleased to acknowledge the helpful discussions during the course of this work with Drs. T. Kubota and T. D. Taylor.

CONTENTS

FIGURES

I. INTRODUCTION

The subject of internal wave generation by a body has been addressed previously by Miles[1], Carrier and Chen[2], and Milder[3]. Each of these authors was concerned primarily with the far-field solutions. Miles used the method of stationary phase to obtain analytic expressions for the far-field internal-wave disturbance in a fluid with a constant Vaisala frequency. Carrier and Chen used similar techniques to obtain a far-field solution in which the Vaisala frequency is constant in a finite thickness layer, and zero elsewhere. Milder solved the problem by numerically inverting the Fourier transform of the solution.

The formulation of the problem used is mathematically equivalent to that of previous authors, except that different dependent variables are used in such a manner that the flow is taken to consist of the sum of rotational and vortical parts. This formulation elucidates both the physics and the mathematics of the problem and suggests an obvious singular perturbation expansion procedure leading to a set of both near-field and far-field equations. While the original equations are a coupled set of two elliptic partial differential equations in three dimensions, the near-field expansion decouples the equations so that the dependent variables may be solved sequentially rather than simultaneously. In addition, the density gradient terms appear only in the inhomogeneous terms of the near-field equations, allowing one to use simple superposition methods to generate near-field solutions for arbitrary thermoclines. The far-field equations are also

---

[1] Miles, J. W., "Internal Waves Generated by a Horizontally Moving Source," Geophysical Fluid Dynamics, 2, 1971, pp. 63-87.

[2] Carrier, G. F., and A. Chen, "Internal Waves Produced by Underwater Vehicles," Report 182-6001-RO-00, TRW Systems, Redondo Beach, Calif., November 1971.

[3] Milder, M., "Internal Waves Radiated by a Moving Source," Report 2702-007, R&D Associates, Santa Monica, Calif., February 1974.

simplified - they are found to be elliptic in only two dimensions and wavelike in the direction of freestream flow. The derivation of these equations is given in Section II.

As indicated by the title, this report considers only the solutions to the near-field equations. Analytic solutions to the near-field equations are given in Section III for the case of a constant Vaisala frequency in some finite region, and zero elsewhere. The solutions in Section III include the potential flow, the first perturbation due to stratification (interval wave), and the first perturbation due to the presence of a free surface (gravity wave).

One new result of this study is a breakdown in the vicinity of the body of the usual slender body assumption. This breakdown results in a singularity behind the body which extends to infinity. Section IV discusses the origin of this breakdown and outlines a technique for obtaining a set of equations which does not have an anomalous solution. The impact of the singularity on the predicted surface disturbance is also discussed.

Section V presents, in graphical form, some typical surface currents obtained from the lengthy equations derived in Section III.

II. PROBLEM FORMULATION

Consider the disturbance created by a slender body moving at constant velocity U_∞ in an inviscid stratified, infinitely deep fluid with negligible surface tension. Eulerian coordinates fixed in the body will be used so the flow is steady. The body will be represented by one source sink singularity pair. This is largely a matter of algebraic convenience; the solution for any body or wake which may be described by some distribution of singularities may be obtained from the source sink solution because of the linearity of the problem.

The basic conservation equations are conservation of mass

$$\nabla \cdot (\rho \overline{V}) = 0 \tag{1}$$

and conservation of momentum

$$(\overline{V} \cdot \nabla)\, \overline{V} + \nabla p/\rho + g\, \overline{i}_z = 0 \tag{2}$$

In addition, in incompressible flow each fluid particle has a density which remains constant as the particle travels along streamlines.

$$(\overline{V} \cdot \nabla)\rho = 0 \tag{3}$$

The boundary condition at the free surface is constant pressure.

At this point, it is convenient to introduce the vorticity

$$\overline{\omega} = \nabla \times \overline{V} \tag{4}$$

The equation governing the production of vorticity may be obtained by taking the curl of the momentum Eq. (2) combined with Eqs. (1) and (3)

$$(\overline{V} \cdot \nabla)\overline{\omega} - (\overline{\omega} \cdot \nabla)\overline{V} + \nabla\left(\frac{1}{\rho}\right) \times \nabla p = 0 \tag{5}$$

The physical motivation for the introduction of the vorticity is as follows. Near the body the flow field is approximately a potential flow. However, the perturbed density field created by this potential flow interacts with the pressure field associated with the thermocline through the last term in Eq. (5) to generate vorticity. Once generated, this vorticity is convected downstream by the flow field. Furthermore, Saffman[4] has shown that a concentrated vortex pair will oscillate in a stratified medium. In the present case, it is assumed that the vorticity will remain distributed throughout the flow rather than rolling up into two concentrated vortices. However, each pair of vortex filaments in the flow field should oscillate in a manner qualitatively similar to the oscillation found by Saffman, and a sum of all these oscillations acting together should provide a description of the internal wave.

There are several small parameters which may be used to linearize the preceding nonlinear equations. These small parameters will be introduced into the equations one at a time for clarity. In the so-called slender body approximation, it is assumed that all perturbations of the flow variables from their nominal values (at upstream infinity) are small. Thus, define the following first order quantities as perturbations about the nominal velocity U_∞, pressure $p_o(z)$, and density $\rho_o(z)$.

$$\overline{V} = (U_\infty + u, v, w) \tag{6}$$

$$p = p_o(z) + p_1 \tag{7}$$

$$\rho = \rho_o(z) + \rho_1 \tag{8}$$

[4] Saffman, P. G., "The Motion of a Vortex Pair in a Stratified Atmosphere," Studies in Applied Math, LI(2), June 1972, pp. 107-119.

Combining Eqs. (1) and (3) and substituting in Eq. (6) gives one

$$u_x + v_y + w_z = 0 \tag{9}$$

The linearized versions of Eqs. (2), (3) and (5) are

$$U_\infty \frac{\partial \bar{V}}{\partial x} + \nabla p_1/\rho_0 + \rho_1 g \bar{i}_z/\rho_0 = 0 \tag{10}$$

$$U_\infty \frac{\partial \rho_1}{\partial x} + w \frac{d\rho_0}{dz} = 0 \tag{11}$$

$$U_\infty \frac{\partial \bar{\omega}}{\partial x} - \frac{1}{\rho_0^2}\left[\frac{d\rho_0}{dz}\bar{i}_z \times \nabla p_1 + \nabla \rho_1 \times \frac{dp_0}{dz}\bar{i}_z\right] = 0 \tag{12}$$

and both vorticity production terms in Eq. (12) are the cross-product of a vector in the z direction with a general three-dimensional vector. Thus, the vorticity can have non-zero components in the x and y directions only. This fact, together with the definition of the vorticity, Eq. (4), implies that the x and y components of the velocity vector are derivable from a potential. The z component of velocity consists of a linear combination of a potential velocity and a rotational velocity, Ω. Thus, Eq. (6) is replaced with

$$\bar{V} = (U_\infty + \phi_x, \phi_y, \phi_z + \Omega) \tag{13}$$

where Ω has two physical interpretations. Besides being the vortical part of the w velocity, it is also a vorticity function from which the two-dimensional vorticity vector may be obtained by differentiation. (It is analogous to the stream function in two-dimensional flow.) Therefore, the vorticity components are given by

$$\bar{\omega} = (\xi, \eta, \zeta) = (\Omega_y, -\Omega_x, 0) \tag{14}$$

Substituting Eqs. (13) and (14) into the y component of Eq. (12) and eliminating p_1 and ρ_1 using Eqs. (10) and (11) gives one

$$- U_\infty \eta_x = U_\infty \Omega_{xx} = \frac{g}{U_\infty} \frac{d \ln \rho_0}{dz} \left(\phi_z + \Omega + \frac{U_\infty^2}{g} \phi_{xx} \right) \qquad (15)$$

Although various substitutions have been made, Eq. (15) has the same physical significance as Eq. (12). The left side of Eq. (15) is the convective derivative [approximated via the slender body assumption as $U_\infty (\partial/\partial x)$] of the y component of vorticity. The right side of Eq. (15) is composed of the vorticity production terms. The importance of the physical basis for this equation will become apparent subsequently.

Following Miles[1], it is convenient to introduce what could be termed a Vaisala wave number k

$$k^2 = k^2(z) = N^2/U_\infty^2 = - \frac{g}{U_\infty^2} \frac{d \ln \rho_0}{dz} \qquad (16)$$

where N is the Vaisala frequency.

A combination of Eqs. (13) and (9) and of Eqs. (15) and (16) gives the basic set of equations considered herein.

$$\phi_{xx} + \phi_{yy} + \phi_{zz} + \Omega_z = 0 \qquad (17)$$

$$\Omega_{xx} + k^2 (\phi_z + \Omega + U_\infty^2 \phi_{xx}/g) = 0 \qquad (18)$$

To these equations must be added the isobaric surface boundary condition. Inspection of Eq. (5) shows this is equivalent to requiring the vorticity components tangent to the free surface to be zero. In the context of the present

slender body approximation this means that Ω is zero at the surface. Thus, from Eq. (15) the surface boundary condition on ϕ is

$$\phi_z + U_\infty^2 \phi_{xx}/g = 0 \tag{19}$$

This completes the derivation of the equations subject to the slender body assumption. Although the equations are now linear, they are still difficult to solve, and it is convenient to take advantage of the additional small parameters. Both the internal waves (characterized by k^2) and the gravity waves (characterized by U_∞^2/g) are assumed to be small compared to the potential flow associated with the body. (Alternatively, the Vaisala length squared, $1/k^2$, is large compared to the body length squared, and U_∞^2/g is small compared to the depth of the body.) Accordingly, the equations will be further linearized in both these parameters. (If the terms involving U_∞^2/g are set to zero, then the preceding equations are equivalent to those considered in Refs. 1, 2 and 3). In the near field [$x < 0(1/k)$] the potential may be split into the following three terms, identified respectively with the body, the internal wave, and the gravity wave.

$$\phi = \phi_0 + \frac{U_\infty^2}{g} \phi_G + k_0^2 \phi_I + \text{higher order terms} \tag{20}$$

where k_0 is a typical value of $k(z)$.

The vorticity is first order and is associated only with the internal wave.

$$\Omega = k_0^2 \Omega_I + \text{higher order terms} \tag{21}$$

Substitution of Eqs. (20) and (21) into the basic set Eqs. (17), (18) and (19) gives

$$\nabla^2 \phi_0 = 0; \; \phi_{0z}(\text{surface}) = 0 \tag{22}$$

$$\nabla^2 \phi_G = 0;\ \phi_{Gz} = -\phi_{0xx}(\text{surface}) \tag{23}$$

$$\Omega_{Ixx} = -(k/k_0)^2 \phi_{0z};\ \Omega_I = \Omega_{Ix} = 0,\ x \to -\infty \tag{24}$$

$$\nabla^2 \phi_I = -\Omega_{Iz};\ \phi_{Iz}(\text{surface}) = 0 \tag{25}$$

where the upstream boundary conditions on Ω_I are such that the freestream vorticity (internal wave) is zero.

Note that the linearization has decoupled the equations, and they may be solved sequentially rather than requiring a simultaneous solution. The internal wave and gravity wave problems are, of course, completely independent to first order, and either one may be obtained without the other.

Far downstream of the body the zero order body potential will decay, and only the first order vorticity (which is convected downstream) will remain. Thus, the highest terms in both potential flow and vortical flow will be $0(k_0^2)$; consequently, a different expansion is required far downstream of the body. The far-field equations [$x > 0(1/k)$] are given here for completeness, even though only the near-field equations [$x < 0(1/k)$] are solved. (It will be shown that the slender body linearization as given is also not uniformly valid.) To obtain the outer expansion, it is necessary to rescale x in the form

$$X = k_0 x \tag{26}$$

Thus, Eqs. (17) and (18) become, to first order

$$k_0^2 \phi_{XX} + \phi_{yy} + \phi_{zz} + \Omega_z = 0 \tag{27}$$

$$\Omega_{XX} + (k/k_0)^2 (\phi_z + \Omega) = 0 \tag{28}$$

In the far field, both the potential and the vorticity are first order

$$\phi = k_0^2 \Phi_1 \tag{29}$$

$$\Omega = k_0^2 \Theta_1 \tag{30}$$

Substitution of Eqs. (29) and (30) and linearization completes the specification of the problem considered.

$$\Phi_{1yy} + \Phi_{1zz} + \Theta_{1z} = 0 \tag{31}$$

$$\Theta_{1XX} + (k/k_0)^2 (\Phi_{1z} + \Theta_1) = 0 \tag{32}$$

The initial conditions for Φ_1 and Θ_1 at $X = 0$ are obtained in the usual way (see Van Dyke[5]) as the limits of ϕ_I and Ω_I as $x \to \infty$.

[5] Van Dyke, M., Perturbation Methods in Fluid Mechanics, Academic Press, New York, 1964.

III. NEAR-FIELD SOLUTION

A. POTENTIAL FLOW SOLUTION

As stated previously, only a simple body represented by a source sink pair will be considered. In addition, it is assumed that the fluid is infinitely deep. These assumptions are not fundamental but are made primarily to simplify the algebra.

The solution to Eq. (22), neglecting the boundary condition, for a single source at the origin in an infinite medium is

$$S(x,y,z) = \frac{-m}{4\pi(x^2+y^2+z^2)^{1/2}} \tag{33}$$

Thus the solution to Eq. (22) (including the surface boundary condition) for a source sink pair on the axis at $x = \pm\ell$ in a fluid of depth d may be obtained by the method of images

$$\phi_0 = S(x+\ell,y,z) - S(x-\ell,y,z) + S(x+\ell,y,z-2d) - S(x-\ell,y,z-2d) \tag{34}$$

B. GRAVITY WAVE SOLUTION

A convenient way to solve Eq. (23) is to transform the problem into one with cylindrical symmetry about the vertical axis. This may be done by defining a new dependent variable ψ such that

$$\phi_G = \psi_{xx} \tag{35}$$

and by considering only a single source-image pair of the zero order potential. Thus, in place of Eq. (23), the following problem is considered:

$$(r\psi_r)_r/r + \psi_{zz} = 0;\ \psi_z(r,d) = 2S(x,y,d) \tag{36}$$

where $r = (x^2 + y^2)^{1/2}$ has been substituted to emphasize the cylindrical symmetry of the problem. Equation (36) is now amenable to treatment with Hankel transforms given by

$$\Psi(R, z) = \int_0^\infty r\, \psi(r, z)\, J_0(rR)dr \tag{37}$$

with the following similar form for the inversion

$$\psi(r, z) = \int_0^\infty R\, \Psi(R, z)\, J_0(rR)dR \tag{38}$$

The problem formulation in Fourier space may be obtained by combining Eqs. (36) and (37)

$$\Psi_{zz} - R^2\Psi = 0;\ \Psi_z(R, d) = \frac{m}{R} e^{-Rd};\ \Psi(R-\infty) = 0 \tag{39}$$

The solution of this equation is

$$\Psi = \frac{m}{R^2} \exp\left[-R(2d-z)\right] \tag{40}$$

and the corresponding solution in physical space is

$$\psi = \frac{-m}{2\pi} \ln \left| 2d-z + \left[x^2 + y^2 + (2d-z)^2\right]^{1/2} \right| \tag{41}$$

To obtain the solution to Eq. (23) associated with a single source-image pair, differentiate Eq. (41) twice with respect to x.

$$G(x, y, \alpha) = \frac{-m}{2\pi} \frac{\alpha\left[y^2 + \alpha^2\right] + \left(x^2 + y^2 + \alpha^2\right)^{1/2} \left(y^2 + \alpha^2 - x^2\right)}{\left(x^2 + y^2 + \alpha^2\right)^{3/2} \left[\alpha + \left(x^2 + y^2 + \alpha^2\right)^{1/2}\right]^2} \tag{42}$$

where α has been substituted for 2d - z.

The complete solution to Eq. (23) for ϕ_0 given by a source sink pair and an image pair above the surface is by superposition

$$\phi_G = G(x+\ell, y, 2d-z) - G(x-\ell, y, 2d-z) \tag{43}$$

C. INTERNAL WAVE SOLUTION (NEAR FIELD)

Since k is a function of z only, the general solution to Eq. (24) may be obtained in analytic form for an arbitrary thermocline. Carrying out the z differentiation and the two x integrals on a potential which consists of a source sink pair and an image pair gives one

$$\Omega_I = (k/k_0)^2 \left[W(x, y, z) + W(x, y, z-2d)\right]; \; d \le z \le -\infty \tag{44}$$

where W is defined by

$$W(x, y, z) = -\frac{mz}{4\pi(y^2 + z^2)} \left| 2\ell + \right.$$

$$\left. \left[(x+\ell)^2 + y^2 + z^2\right]^{1/2} - \left[(x-\ell)^2 + y^2 + z^2\right]^{1/2} \right| \tag{45}$$

The preceding expression is zero for $x \to -\infty$ corresponding to the assumption of zero vorticity or no internal wave upstream. As $x \to \infty$, the vorticity being generated by the body potential goes to zero and Eq. (45) approaches a function of y and z only. It should be noted that if $k(0) \neq 0$, then the vorticity is singular on the axis $y=z=0$ behind the body. This behavior arises from the fact that the slender body linearization is not uniformly valid. This will be discussed further in Section IV.

The complete solution to Eq. (24) includes the vorticity generated by the body source sink pair plus the vorticity generated by the image sources. If the body and the thermocline are well below the surface, the vorticity generated by the image sources will be negligible.

Equation (44) gives the vorticity distribution beneath the free surface. Note that if the method of images is used to solve Eq. (25), the image vorticity distribution above the free surface will be required to satisfy the free surface boundary condition on ϕ_I.

The solution for ϕ_I is obtained using a method analogous to that used to obtain ϕ_G. First, define a new dependent variable χ such that

$$\chi = \phi_{Ixx} \tag{46}$$

This definition combined with Eqs. (24) and (25) results in the following equation for χ

$$\nabla^2 \chi = \frac{\partial}{\partial z}\left[(k/k_0)^2 \phi_{0,z}\right] \tag{47}$$

This problem, like Eq. (36), is axisymmetric about the vertical axis if ϕ_0 consists only of sources placed along the z axis. Thus, Eq. (47) may also be solved by Hankel transforms.

If the functional form of the thermocline represented here by k(z) is simple, then analytic expressions for x can be obtained. In general, the thermocline is quite complicated and some sort of numerical solution is required. It is not suggested that Eq. (47) be transformed, solved numerically using a given k(z), and then inverted numerically, but rather that k(z) be idealized as a piecewise constant function so that analytic solutions to Eq. (47) may be obtained for each constant value of k. The total solution is then obtained by either analytically or numerically summing up the solutions due to each constant piece of k(z).

Accordingly, Eq. (47) will be solved for

$$\phi_0 = S(x, y, z) \tag{48}$$

and

$$k = k_0;\ L_1 \le z \le L_2$$
$$k = 0;\ \text{elsewhere} \tag{49}$$

The solution for the body in the thermocline region ($L_1 \le 0 \le L_2$) is then χ_1 where

$$\chi_1 = \frac{mL_1 z}{8\pi(x^2+y^2+z^2)^{3/2}} + \frac{S(x,y,z)}{4} - \frac{S(x,y.2L_2-z)}{4};\ -\infty \le z \le L_1 \tag{50}$$

$$\chi_1 = \frac{mz^2}{8\pi(x^2+y^2+z^2)^{3/2}} + \frac{S(x,y,z)}{2} - \frac{S(x,y,2L_1-z)}{4} - \frac{S(x,y,2L_2-z)}{4};$$

$$L_1 \le z \le L_2 \tag{51}$$

$$\chi_1 = \frac{mL_2 z}{8\pi(x^2+y^2+z^2)^{3/2}} + \frac{S(x,y,z)}{4} - \frac{S(x,y,2L_1-z)}{4};\ L_2 \le z \le \infty \tag{52}$$

The solution to Eqs. (47) through (49) for the single source in the thermocline is given in Eqs. (50) through (52). The solution to the same set of equations for the case in which the body is below the thermocline ($0 \le L_1 \le L_2$) is as follows:

$$\chi_2 = \frac{S(x,y,2L_1-z)}{4} - \frac{S(x,y,2L_2-z)}{4};\ -\infty \le z \le L_1 \tag{53}$$

$$\chi_2 = \frac{mz(z-L_1)}{8\pi(x^2+y^2+z^2)^{3/2}} + \frac{S(x,y,z)}{4} - \frac{S(x,y,2L_2-z)}{4};\ L_1 \le z \le L_2 \tag{54}$$

$$\chi_2 = \frac{m(L_2-L_1)z}{8\pi(x^2+y^2+z^2)^{3/2}};\ L_2 \le z \le \infty \tag{55}$$

If a pair of solutions χ_1 are superposed (corresponding to a source sink pair) and the two x integrations are carried out, subject to the conditions that all velocities are zero at $x = -\infty$, the result is

$$\frac{8\pi F_1(x, y, z, L_1, L_2)}{m} = \frac{2\ell L_1 z}{y^2 + z^2} + \frac{\ell}{2} \ln \frac{y^2 + z^2}{y^2 + [2L_2 - z]^2}$$

$$+ \frac{L_1 z}{y^2 + z^2} \left\{ \left([x+\ell]^2 + y^2 + z^2 \right)^{1/2} - \left([x-\ell]^2 + y^2 + z^2 \right)^{1/2} \right\}$$

$$+ \frac{x+\ell}{2} \left\{ \sinh^{-1} \left[\frac{x + \ell}{(y^2 + [2L_2 - z]^2)^{1/2}} \right] \right.$$

$$\left. - \sinh^{-1} \left[\frac{x + \ell}{(y^2 + z^2)^{1/2}} \right] \right\}$$

$$- \frac{x-\ell}{2} \left\{ \sinh^{-1} \left[\frac{x - \ell}{(y^2 + [2L_2 - z]^2)^{1/2}} \right] \right.$$

$$\left. - \sinh^{-1} \left[\frac{x - \ell}{(y^2 + z^2)^{1/2}} \right] \right\}$$

$$+ \frac{1}{2} \left\{ \left([x+\ell]^2 + y^2 + z^2 \right)^{1/2} - \left([x-\ell]^2 + y^2 + z^2 \right)^{1/2} \right.$$

$$- \left([x+\ell]^2 + y^2 + [2L_2 - z]^2 \right)^{1/2}$$

$$\left. + \left([x-\ell]^2 + y^2 + [2L_2 - z]^2 \right)^{1/2} \right\} ; \quad -\infty \le z \le L_1 \qquad (56)$$

$$\frac{8\pi F_1(x,y,z,L_1,L_2)}{m} = \frac{z^2}{y^2+z^2}\left\{\left([x+\ell]^2+y^2+z^2\right)^{1/2} - \left([x-\ell]^2+y^2+z^2\right)^{1/2}\right\}$$

$$+ \frac{2\ell z^2}{y^2+z^2} + \frac{\ell}{2}\left\{\ln\frac{y^2+z^2}{(y^2+[2L_1-z]^2)} + \ln\frac{y^2+z^2}{y^2+[2L_2-z]^2}\right\}$$

$$+ \frac{(x+\ell)}{2}\left\{\sinh^{-1}\left[\frac{x+\ell}{(y^2+[2L_1-z]^2)^{1/2}}\right]\right.$$

$$\left. + \sinh^{-1}\left[\frac{x+\ell}{(y^2+[2L_2-z]^2)^{1/2}}\right] - 2\sinh^{-1}\left[\frac{x+\ell}{(y^2+z^2)}\right]\right\}$$

$$- \frac{x-\ell}{2}\left\{\sinh^{-1}\left[\frac{x-\ell}{(y^2+[2L_1-z]^2)^{1/2}}\right]\right.$$

$$\left. + \sinh^{-1}\left[\frac{x-\ell}{(y^2+[2L_2-z]^2)^{1/2}}\right] - 2\sinh^{-1}\left[\frac{x-\ell}{(y^2+z^2)^{1/2}}\right]\right\}$$

$$+ \frac{1}{2}\left\{2\left([x+\ell]^2+y^2+z^2\right)^{1/2} - \left([x+\ell]^2+y^2+[2L_1-z]^2\right)^{1/2}\right.$$

$$\left. - \left([x+\ell]^2+y^2+[2L_2-z]^2\right)^{1/2}\right\}$$

$$- \frac{1}{2}\left\{2\left([x-\ell]^2+y^2+z^2\right)^{1/2} - \left([x-\ell]^2+y^2+[2L_1-z]^2\right)^{1/2}\right.$$

$$\left. - \left([x-\ell]^2+y^2+[2L_2-z]^2\right)^{1/2}\right\}; \quad L_1 \le z \le L_2 \qquad (57)$$

$$\frac{8\pi F_1(x,y,z,L_1,L_2)}{m} = \frac{2\ell z L_2}{y^2+z^2} + \frac{\ell}{2}\ln\frac{y^2+z^2}{y^2+[2L_1-z]^2}$$

$$+ \frac{L_2 z}{y^2+z^2}\left\{\left([x+\ell]^2+y^2+z^2\right)^{1/2} - \left([x-\ell]^2+y^2+z^2\right)^{1/2}\right\}$$

$$+ \frac{(x+\ell)}{2}\left\{\sinh^{-1}\left[\frac{x+\ell}{(y^2+[2L_1-z]^2)^{1/2}}\right]\right.$$

$$\left. - \sinh^{-1}\left[\frac{x+\ell}{(y^2+z^2)^{1/2}}\right]\right\}$$

$$- \left(\frac{x-\ell}{2}\right)\left\{\sinh^{-1}\left[\frac{x-\ell}{(y^2+[2L_1-z]^2)^{1/2}}\right]\right.$$

$$\left. - \sinh^{-1}\left[\frac{x-\ell}{(y^2+z^2)^{1/2}}\right]\right\}$$

$$+ \frac{1}{2}\left\{\left[(x+\ell)^2+y^2+z^2\right]^{1/2} - \left[(x-\ell)^2+y^2+z^2\right]^{1/2}\right.$$

$$\left. - \left[(x+\ell)^2+y^2+(2L_1-z)^2\right]^{1/2} + \left[(x-\ell)^2+y^2+(2L_1-z)^2\right]^{1/2}\right\};$$

$$L_2 \le z < \infty \qquad (58)$$

Note that F_1 is the ϕ_I solution for a body in a finite, constant thermocline (k = constant) in an infinite medium. That is, no free surface or, alternately, no image sources have been included.

A similar result for the body (source sink pair) below the constant thermocline may be obtained by integrating Eqs. (53) through (55).

$$\frac{16\pi F_2(x,y,z,L_1,L_2)}{m} = \ell \ln \frac{y^2+[z-2L_1]^2}{y^2+[z-2L_2]^2}$$

$$+ (x+\ell)\left\{\sinh^{-1}\left[\frac{x+\ell}{\left(y^2+[z-2L_2]^2\right)^{1/2}}\right]\right.$$

$$\left. - \sinh^{-1}\left[\frac{x+\ell}{\left(y^2+[z-2L_1]^2\right)^{1/2}}\right]\right\}$$

$$- (x-\ell)\left\{\sinh^{-1}\left[\frac{x-\ell}{\left(y^2+[z-2L_2]^2\right)^{1/2}}\right]\right.$$

$$\left. - \sinh^{-1}\left[\frac{x-\ell}{\left(y^2+[z-2L_1]^2\right)^{1/2}}\right]\right\}$$

$$+ \left[(x+\ell)^2+y^2+(z-2L_1)^2\right]^{1/2} - \left[(x+\ell)^2+y^2+(z-2L_2)^2\right]^{1/2}$$

$$- \left[(x-\ell)^2+y^2+(z-2L_1)^2\right]^{1/2} + \left[(x-\ell)^2+y^2+(z-2L_2)^2\right]^{1/2};$$

$$-\infty \le z \le L_1 \qquad (59)$$

$$\frac{8\pi F_2(x,y,z,L_1,L_2)}{m} = \frac{\ell}{2}\ln\frac{y^2+z^2}{y^2+[z-2L_2]^2} + \frac{2\ell z(z-L_1)}{y^2+z^2}$$

$$+\left(\frac{x+\ell}{2}\right)\left\{\sinh^{-1}\left[\frac{x+\ell}{\left(y^2+[z-2L_2]^2\right)^{1/2}}\right] - \sinh^{-1}\left[\frac{x+\ell}{(y^2+z^2)^{1/2}}\right]\right\}$$

$$-\left(\frac{x-\ell}{2}\right)\left\{\sinh^{-1}\left[\frac{x-\ell}{\left(y^2+[z-2L_2]^2\right)^{1/2}}\right] - \sinh^{-1}\left[\frac{x-\ell}{(y^2+z^2)^{1/2}}\right]\right\}$$

$$+\left[(x+\ell)^2+y^2+z^2\right]^{1/2} - \left[(x+\ell)^2+y^2+(z-2L_2)^2\right]^{1/2}$$

$$-\left[(x-\ell)^2+y^2+z^2\right]^{1/2} + \left[(x-\ell)^2+y^2+(z-2L_2)^2\right]^{1/2}$$

$$+\frac{z(z-L)}{y^2+z^2}\left\{\left[(x+\ell)^2+y^2+z^2\right]^{1/2} - \left[(x-\ell)^2+y^2+z^2\right]^{1/2}\right\};$$

$$L_1 \le z \le L_2 \qquad (60)$$

$$\frac{8\pi F_2(x,y,z,L_1,L_2)}{m} = \frac{(L_2-L_1)z}{y^2+z^2}\left\{2\ell + \left[(x+\ell)^2+y^2+z^2\right]^{1/2} - \left[(x-\ell)^2+y^2+z^2\right]^{1/2}\right\};\ L_2 \le z \le \infty \qquad (61)$$

The complete solution to Eq. (25) (including the free surface boundary condition) in terms of the functions defined previously for the body within a finite thermocline is

$$\phi_I = F_1(x,y,z,L_1,L_2) + F_1(x,y,2d-z,L_1,L_2) + F_2(x,y,z,2d-L_2,2d-L_1)$$

$$+ F_2(x,y,2d-z,2d-L_2,2d-L_1);\ L_1 \le 0 \le L_2 \qquad (62)$$

and the general solution for the body outside the thermocline is

$$\phi_I = F_2(x,y,z,L_1,L_2) + F_2(x,y,2d-z,L_1,L_2) + F_2(x,y,z,2d-L_2,2d-L_1)$$

$$+ F_2(x,y,2d-z,2d-L_2,2d-L_1);\ 0 \le L_1 \le L_2 \qquad (63)$$

The last two terms in both Eqs. (62) and (63) may be negligible in most cases of practical interest because of the separation of the thermocline and the sources.

If the thermocline is variable with depth, a solution may be obtained by approximating the thermocline as a piecewise constant function and summing (either analytically or numerically) relevant solutions of Eqs. (62) and (63). One advantage of this method is that the summation need only be carried out for the specific variable of interest at the location of interest. For example, if values of the surface current are required, expressions for the velocity at the surface may be obtained by differentiating Eqs. (62) and (63) and evaluating the result at $z = d$. The numerical quadrature (to take account of the variable density) is then a two-dimensional quadrature to obtain a two-dimensional result.

IV. SINGULARITY BEHIND BODY

The near-field solution, obtained in Section III, was found to be singular on the axis behind the body. This section contains a brief discussion of why the model predicts this physically impossible result, and a procedure is suggested which could correct this deficiency in the model equations.

The source of the singularity may be identified by considering the physical significance of the vorticity Eq. (5). The first term in Eq. (5) is the convective derivative of the vorticity, i.e., the rate of change of the vorticity along streamlines in the flow. The second term is a vortex stretching term which can change the magnitude of the vorticity by stretching individual vortex filaments. The third term in Eq. (5) is a vorticity production term associated with gradients in pressure and density. Now, consider the effect on the vorticity equation of introducing the slender body assumption. The x component of this vector equation is Eq. (15). The convective derivative has become simply the partial derivative with respect to x, the stretching term is higher order and has been dropped, and the production term is given by the right-hand side of Eq. (15).

The cause of the singularity in vorticity on the axis behind the body is now obvious. The vorticity on the streamline should be computed by integrating along the y=z=0 axis upstream of the body, along a body streamline passing over the body, and then along the axis behind the body (for an axisymmetric potential flow). However, in the present slender body model this vorticity is computed by integrating along the axis right through the body. Since in the present case the body is modeled by a source sink pair on the axis, this integration passes through two singular points. Note that previous studies which employ the slender body assumption[1,2,3] suffer from the same deficiency.

The singularity may, in principle, be removed from the solution of the slender body equations by generating a separate expansion valid in the immediate vicinity of the body. The major feature of this near-body expansion is that the convective derivative of the vorticity may be directed along the streamlines of the zero order potential flow which go around the body. Although this step is simple in principle, the resultant equations are quite complex and therefore have not been solved. In addition, it seems pointless to carry out an expansion valid near the body for inviscid flow. In any real fluid, there will also be a boundary layer growing on the body, in which vorticity is diffused away from the wall. An investigation of the flow field near the body which neglects the boundary layer appears to be academic. A consideration of the boundary-layer flow is beyond the scope of the present work.

The typical solutions presented in Section V show that for most practical cases the effect of the singularity in the flow has a negligible effect on the surface solution. Thus, it is concluded that unless there is a specific interest in the flow field in the vicinity of the axis behind the body, the near body expansion outlined in this section is an unnecessary refinement.

V. TYPICAL NEAR-FIELD SURFACE VELOCITIES

This section presents, in graphical form, values of the velocity at the surface for two cases: one in which the body is above the thermocline, and one in which the body is within the thermocline. To simplify interpretation and also to facilitate a comparison with published far-field results[2], only thermoclines which are constant and non-zero in a finite region will be discussed here. (However, it should be noted that non-constant thermoclines may be treated easily by summing or integrating the solutions in Section III. This summation is possible in the near field because the thermocline behavior appears only in the inhomogeneous terms of the inner expansion.)

The relevant physical parameters for the two cases considered are summarized in Table 1. Recall that the body is modeled by a source sink pair and therefore the zero order body shape is a Rankine ovoid (provided the free surface is neglected).

First consider the surface velocity component parallel to the freestream flow, generated by a body above the thermocline (Case 1 in Table 1). The u component of velocity is found to be symmetric in both x and y (the direction of freestream flow and the cross-track direction, respectively). This symmetry applies to both the stratification and free surface perturbations as well as to the zero order potential flow. The stratification contribution to the u velocity goes to zero far downstream because the vorticity generating this disturbance must line up with the freestream far from the body. Figure 1 shows the variation of u with x in the plane directly above the body. (Recall that x=y=0 is directly above the center of the body.) The main contribution to the velocity arises from the potential flow, with a significant correction being made by the stratification contribution. The contribution generated by relaxing the approximation that the free surface is a plane is negligible for a body at this depth. Figures 2, 3 and 4 are plots of u as a function of y at those stations in Fig. 1 where u is nominally a maximum, zero and a minimum. The free surface contribution is so small that it is not included in

Table 1. Physical Parameters

Body Dimensions:	Length = 300 ft Diameter = 30 ft
Thermocline Characteristics:	Top = 164 ft deep Bottom = 492 ft deep $k = 0.002\ ft^{-1}$
Velocity of Body:	5 ft/sec
Case 1. Body Above Thermocline:	Body depth = 145 ft
Case 2. Body In Thermocline:	Body depth = 183 ft

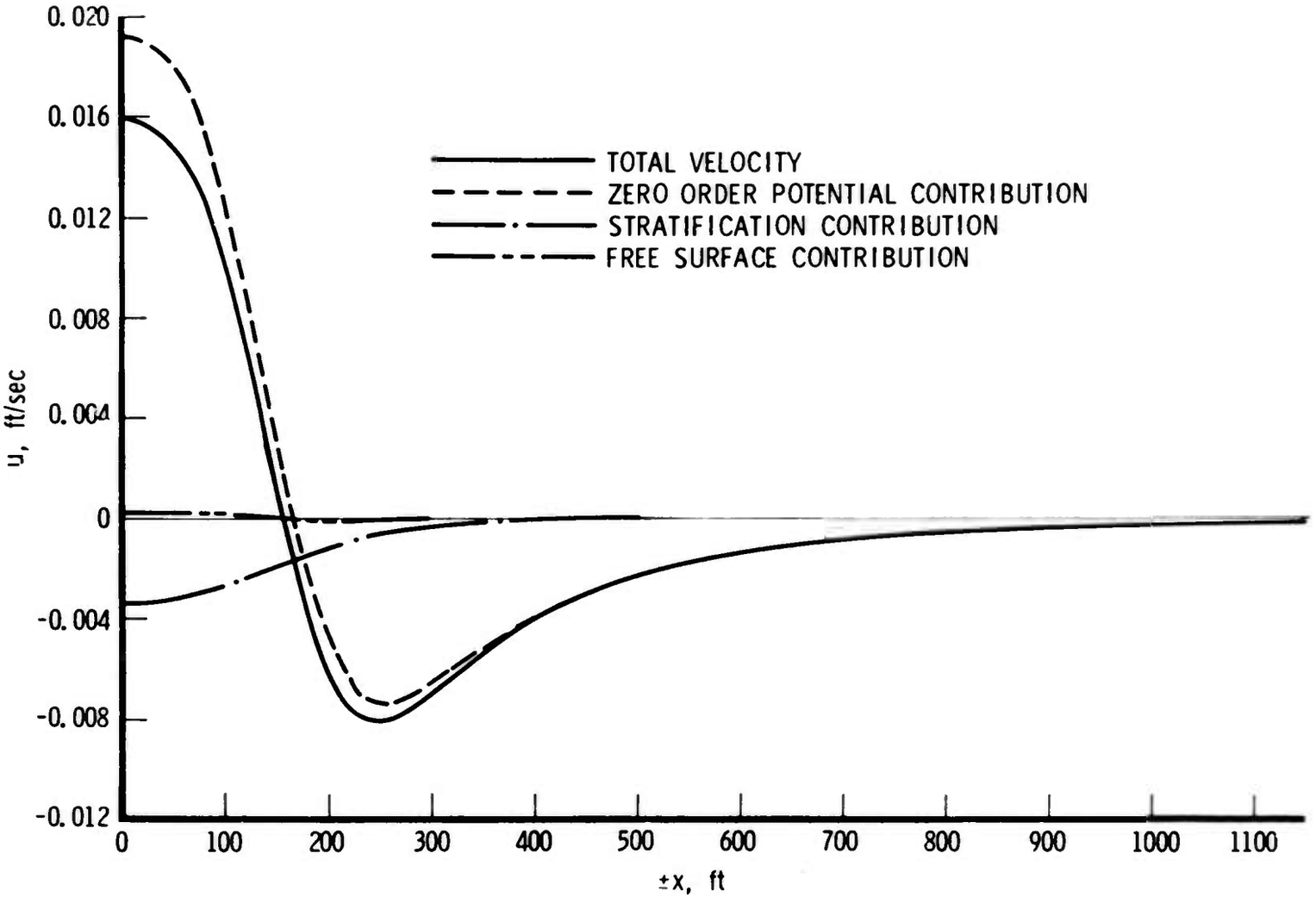

Fig. 1. x-Component of Surface Current in y=0 Plane
(Body Above Thermocline)

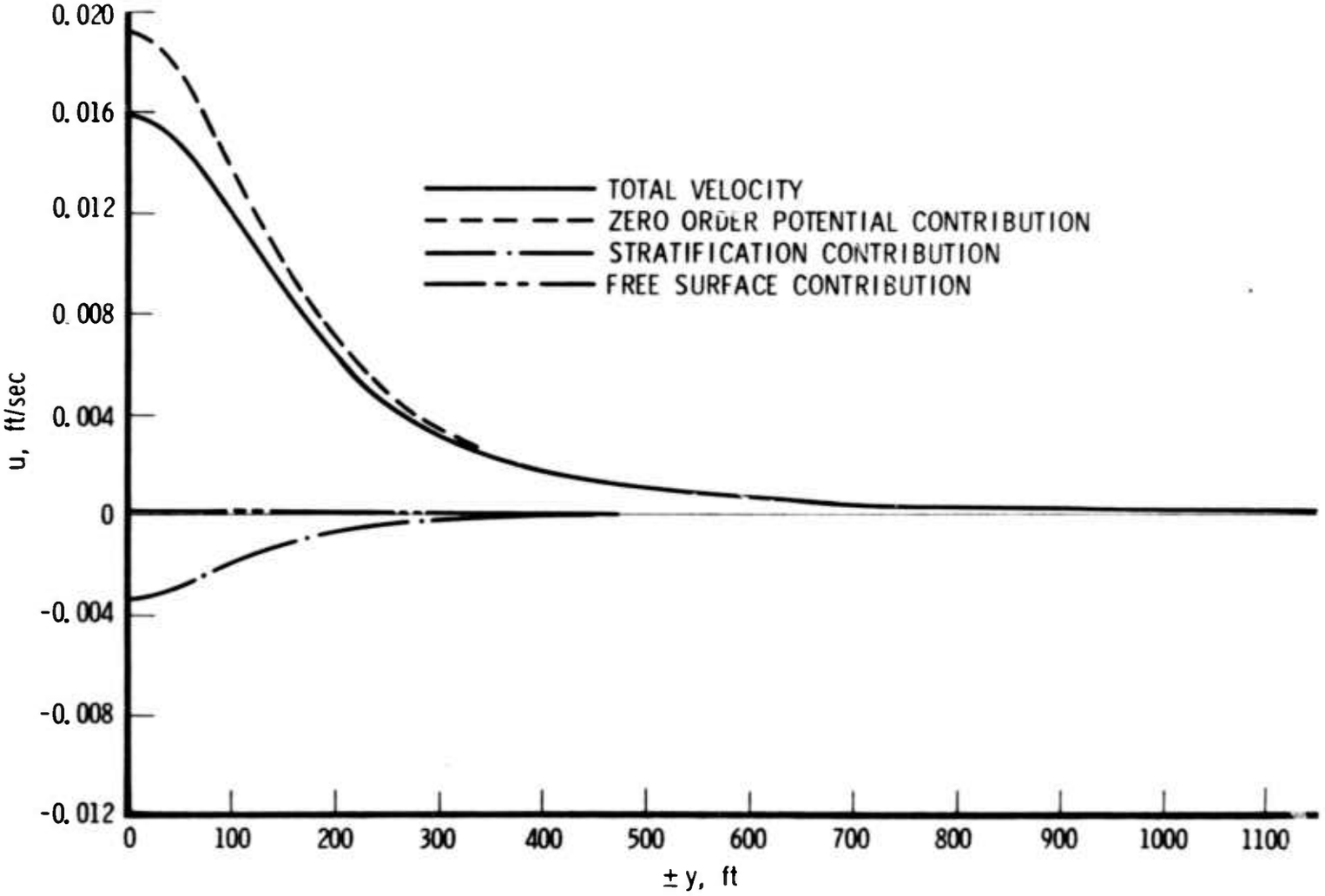

Fig. 2. x-Component of Surface Current in x=0 Plane
(Body Above Thermocline)

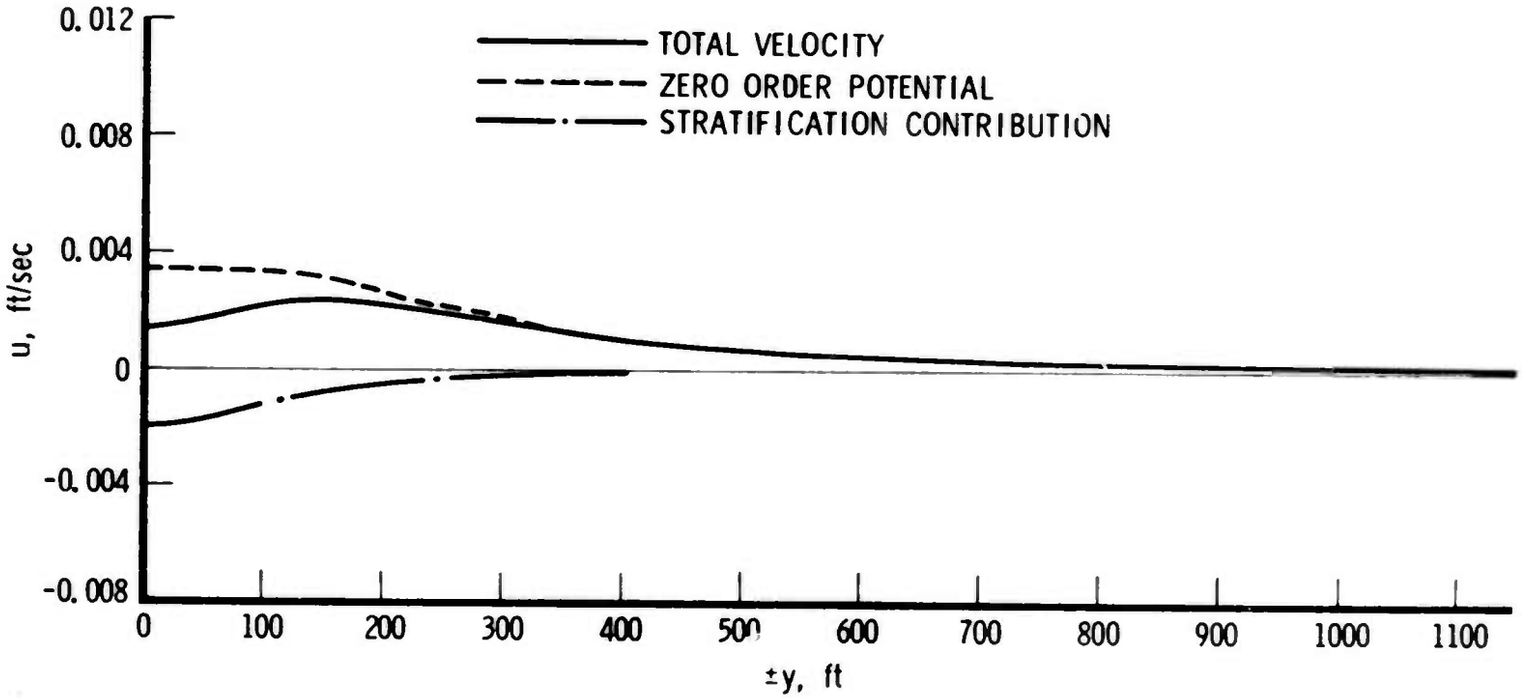

Fig. 3. x-Component of Surface Current in x = ±150-ft Plane (Body Above Thermocline)

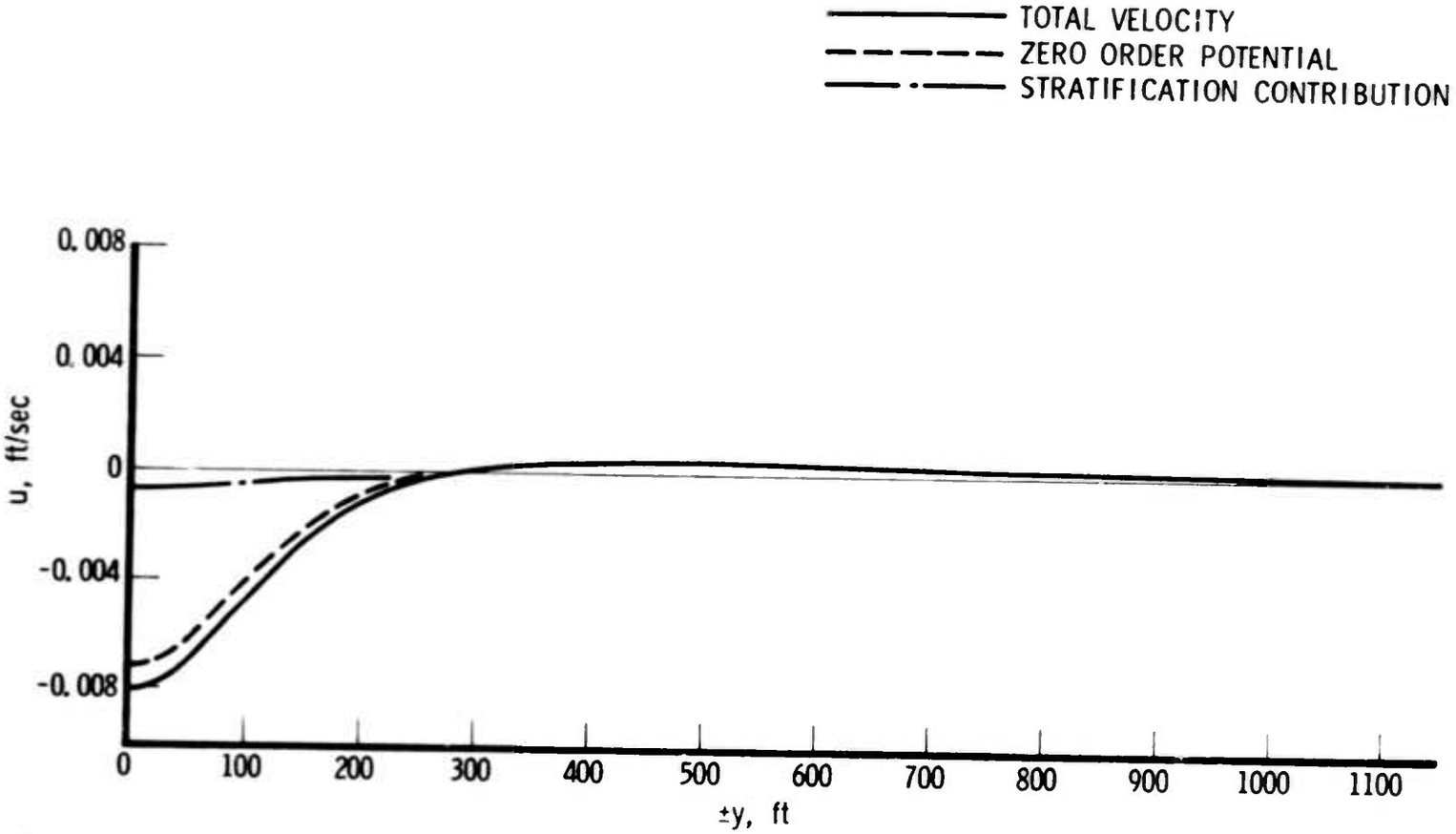

Fig. 4. x-Component of Surface Current in x = ±250-ft Plane (Body Above Thermocline)

figures subsequent to Fig. 2 showing the x and y velocity components. Figures 1 through 4 show that the maximum x component of surface current occurs directly above the center of the body. The maximum negative values are in the y=0 plane and occur about 100 ft fore and aft of the body stagnation points.

Symmetry conditions require that the y component of velocity be identically zero at y=0; thus, Fig. 5 shows the surface cross-track velocity as a function of x at y = 100 ft. This curve shows the expected behavior of zero stratification contribution upstream, growing to some asymptotic value far downstream. This is the expected manifestation of the trailing vorticity which the stratification generates. Figures 6, 7 and 8 show the y velocity component as a function of y at the same x stations behind the body used for the x velocity plots. These figures all indicate that the peak disturbance is about 100 ft from the y=0 plane; thus, Fig. 5 is roughly the peak value of the cross-track velocity as a function of x.

The vertical surface velocity is shown in Figs. 9 and 10. The only contribution to this velocity is the gravity wave contribution and, as previously noted, the magnitude is very small. For bodies closer to the surface, a larger disturbance of the same general character would occur. The peak disturbance occurs on the y=0 axis with a maximum (minimum) velocity almost directly above the aft forward) stagnation point.

Now consider the case of the body in the thermocline. The stratification is unchanged but the body is now 19 ft below the top of the thermocline rather than 19 ft above it. Figures 11 and 12 show the x component of the velocity in the y=0 and x=0 planes, respectively. If these two figures are compared with Figs. 1 and 2, the potential component of the velocity is found to be reduced magnitude and spread out in both the x and y directions for the deeper body. (This is a function of depth only since the zero order potential is independent of stratification.) The stratification contribution to the velocity has the same general behavior as the potential contribution; it is also reduced in magnitude and spread out. Thus, there is no obvious

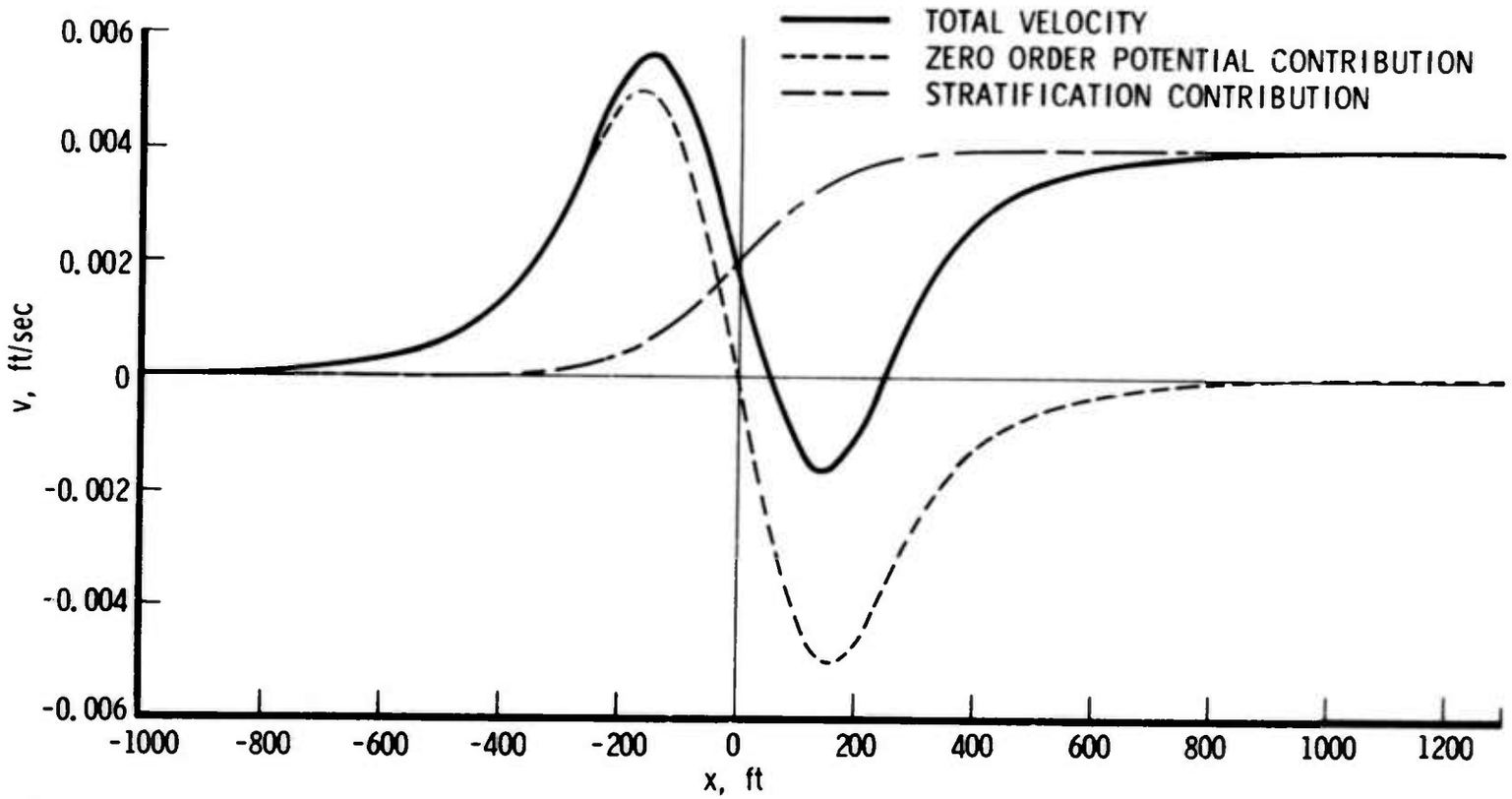

Fig. 5. y-Component of Surface Velocity in y=100-ft Plane (Body Above Thermocline)

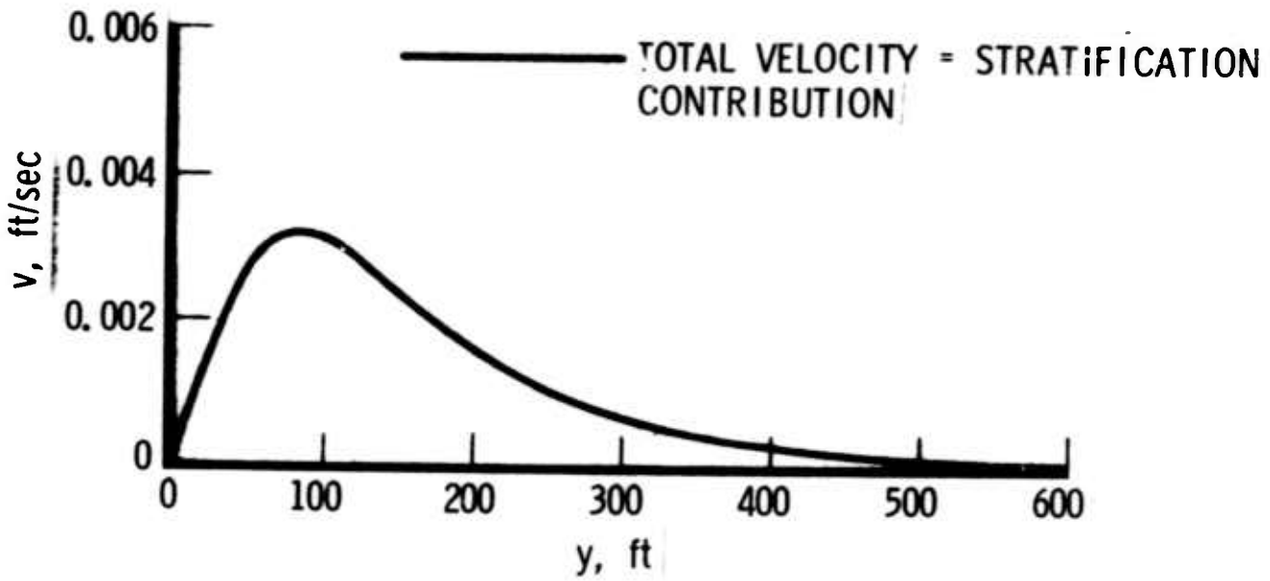

Fig. 6. y-Component of Surface Velocity in x=0 Plane (Body Above Thermocline)

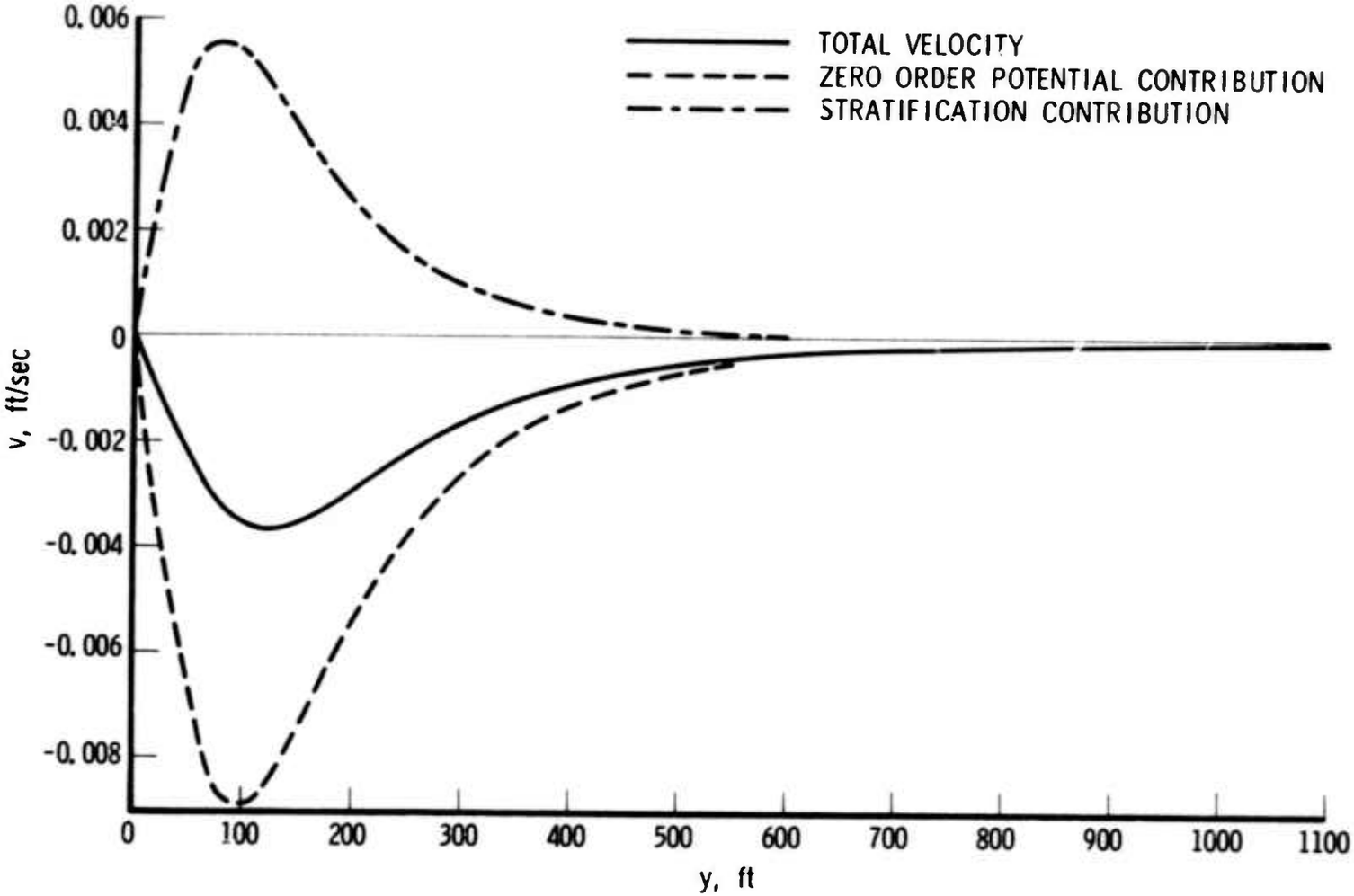

Fig. 7. y-Component of Surface Current in x=150-ft Plane (Body Above Thermocline)

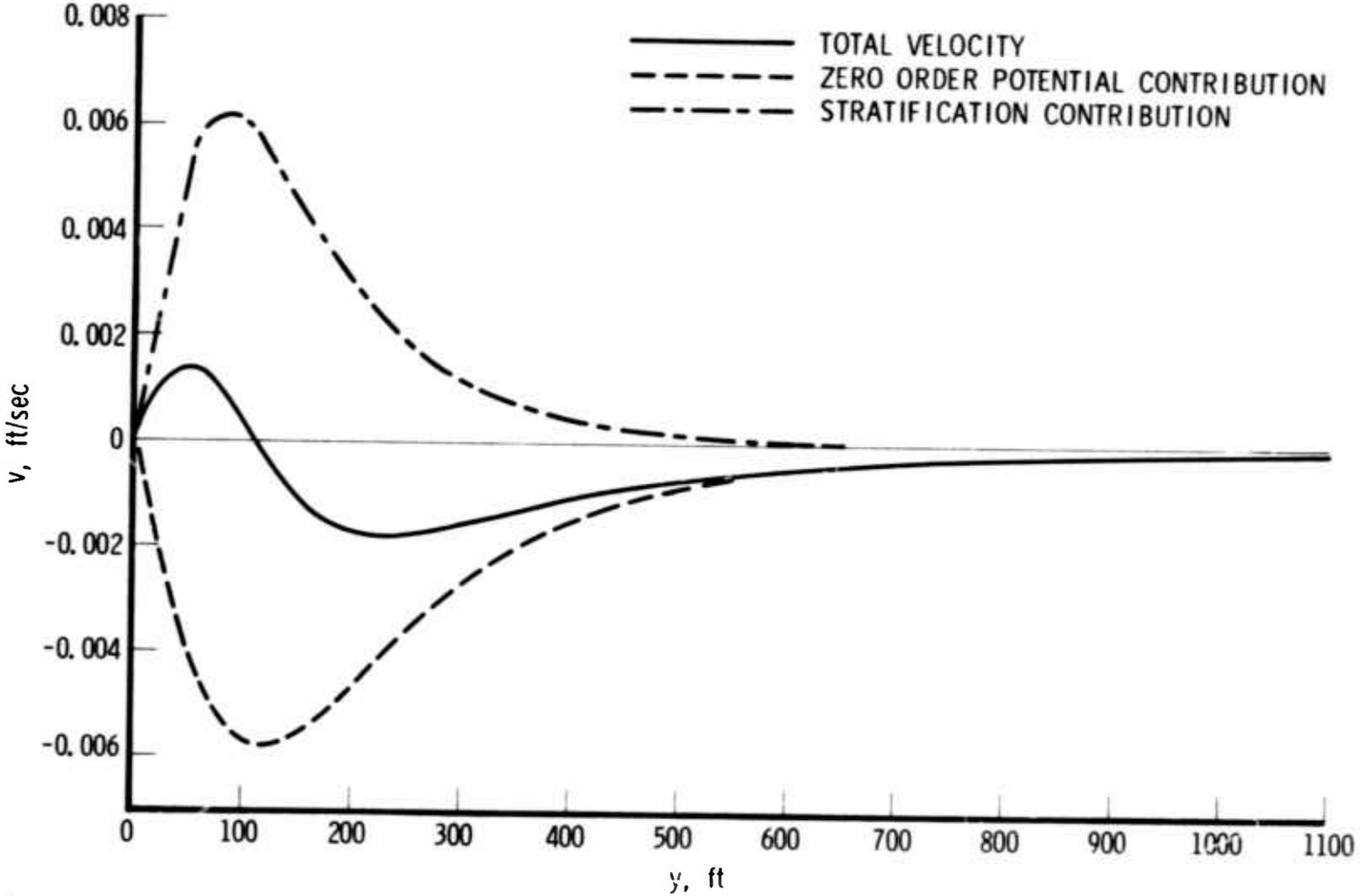

Fig. 8. y-Component of Surface Current in x=250-ft Plane (Body Above Thermocline)

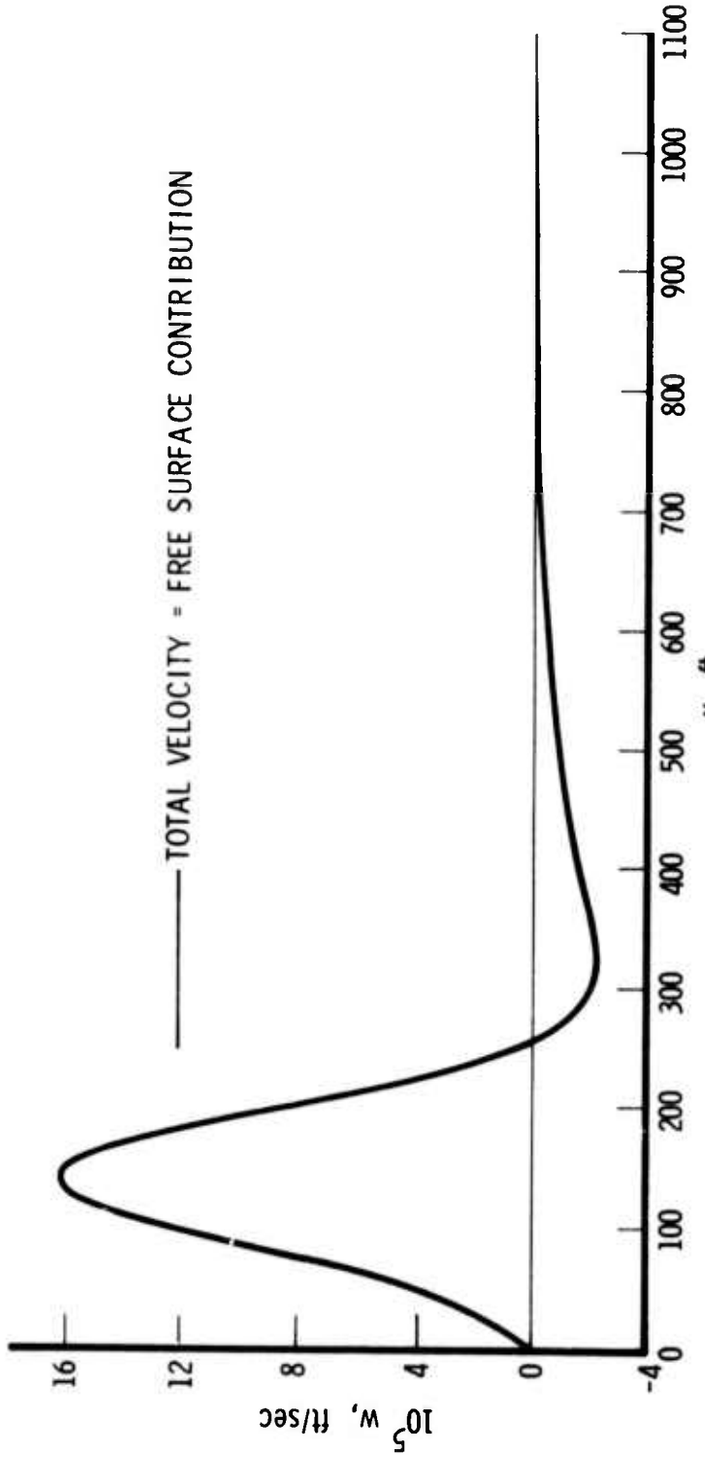

Fig. 9. Vertical, Surface Velocity in y=0 Plane
(Body Above Thermocline)

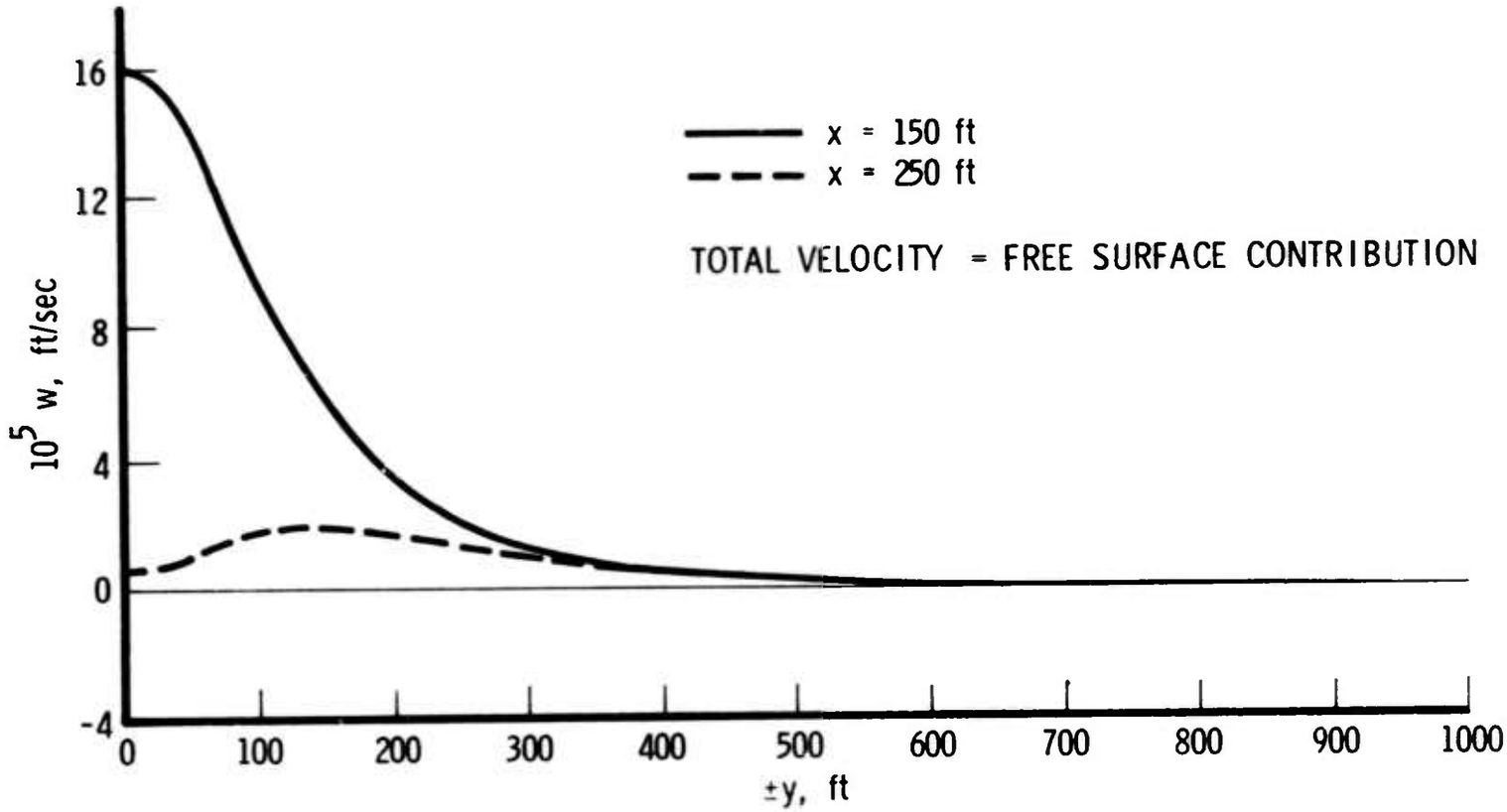

Fig. 10. Vertical, Surface Velocity in x=150- and 250-ft Planes (Body Above Thermocline)

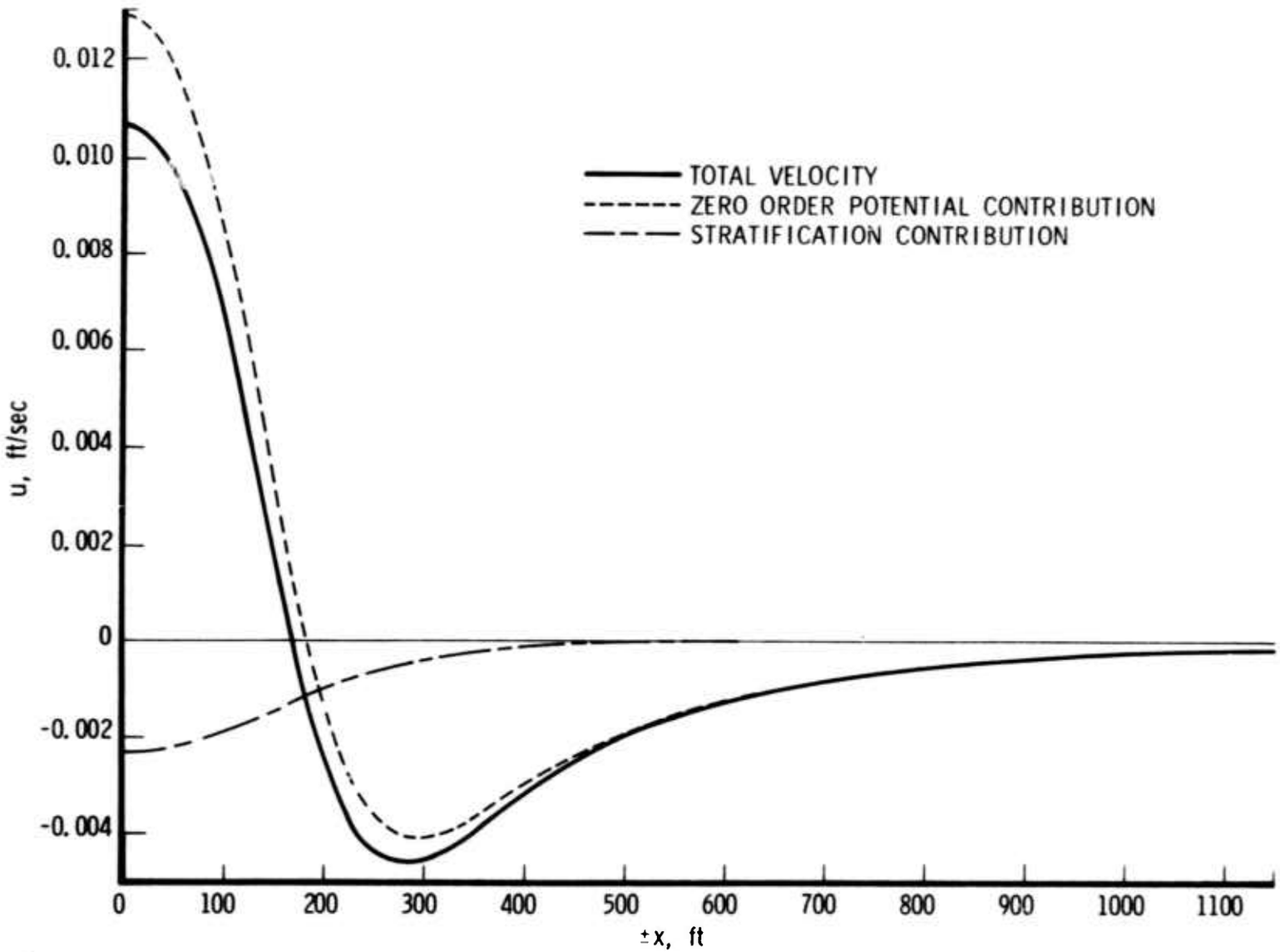

Fig. 11. x-Component of Surface Current in y=0 Plane (Body in Thermocline)

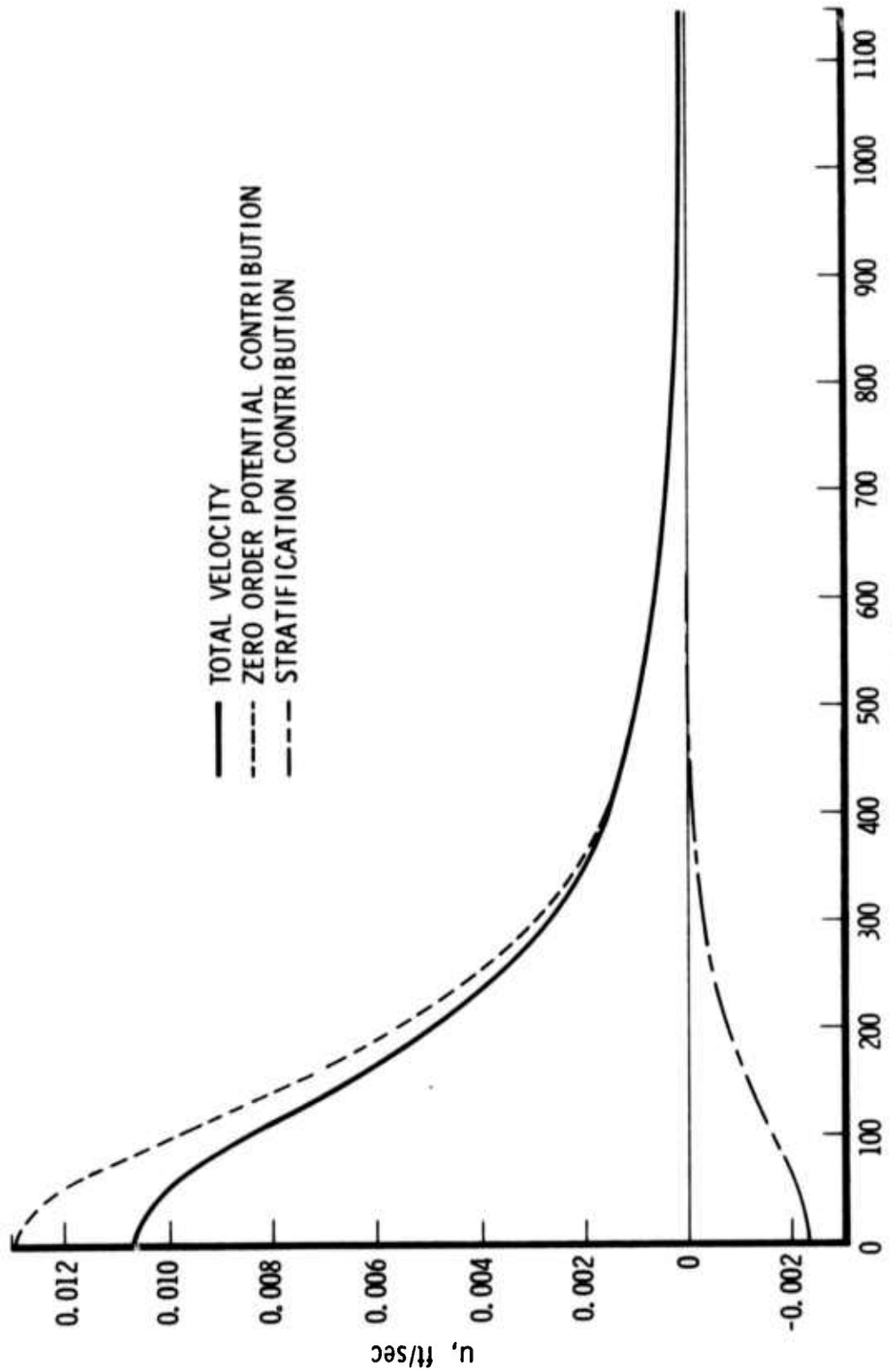

Fig. 12. x-Component of Surface Current in x=0 Plane (Body in Thermocline)

anomalous behavior of the stratification generated velocity associated with the fact that for this case the singularity behind the body is present. Since the stratification contribution to u remains small and well-behaved, it is concluded that the total velocity predictions in Figs. 11 and 12 are realistic and accurate values.

Figures 13 and 14 are typical plots of the y component of surface velocity for the body in the thermocline. A comparison of these curves with Figs. 5 and 6 shows decreased velocities and spreading in the y direction. Again, there are no obvious anomalies, and the similarity of the two sets of curves lends credence to present predictions. However, for the y component of the velocity, the total velocity is the stratification contribution far downstream. Thus, an error caused by the singularity is more important here. To further study the effect of the singularity in the thermocline, the contribution to the present surface current from the thermocline layer one body diameter thick (30 ft) centered at the body was computed. The contribution of this stratified layer to the velocities in Figs. 11 through 14 is slightly less than ten percent of the given stratification contribution. This represents an upper bound on the possible error associated with the singularity. The contribution of the singularity should properly be removed by cutting out a circular region about the axis; the present calculation cut out the plane region bounded by $y = \pm 15$ ft. It is therefore concluded that Figs. 13 and 14 are valid predictions of the surface velocity, and any error associated with the singularity is expected to be substantially less than ten percent of the values shown.

Figure 15 is a semi-logarithmic plot of the curve illustrated in Fig. 14. The log scale more clearly shows that v asymptotes to zero from negative values. (Computations were made much farther out in y than are shown and no further zeros were found.) The stratification contribution to u also has zero crossings as a function of both x and y, although these are not discernible on the scale of Figs. 11 and 12. One further point should be noted; the value of v for the symmetric bodies considered here at x=0 is exactly half the asymptotic value as $x \to \infty$. Thus, Figs. 6, 14 and 15 can be interpreted as plots of $v/2$ for $x \to -\infty$.

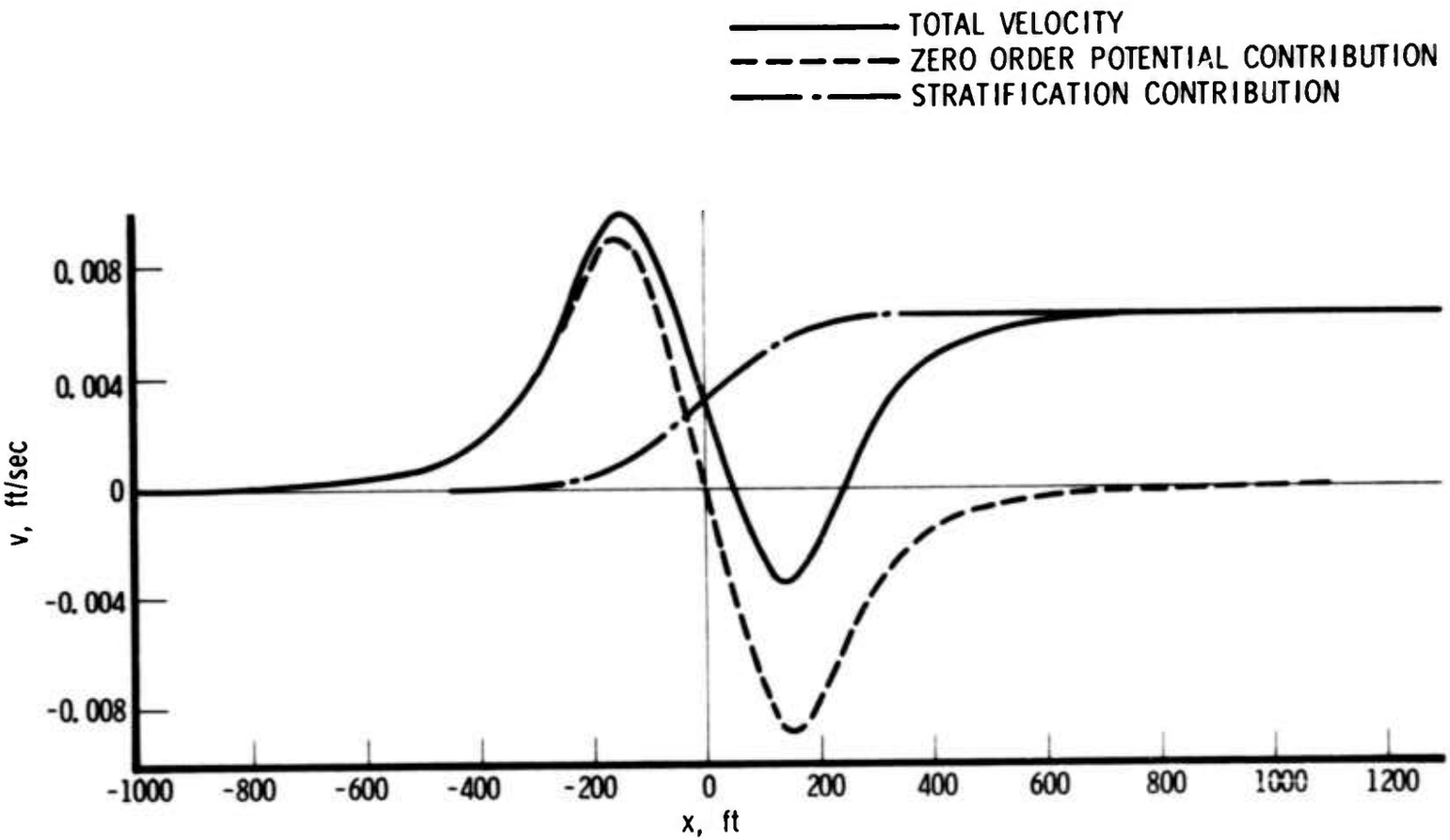

Fig. 13. y-Component of Surface Velocity in y=100-ft Plane (Body in Thermocline)

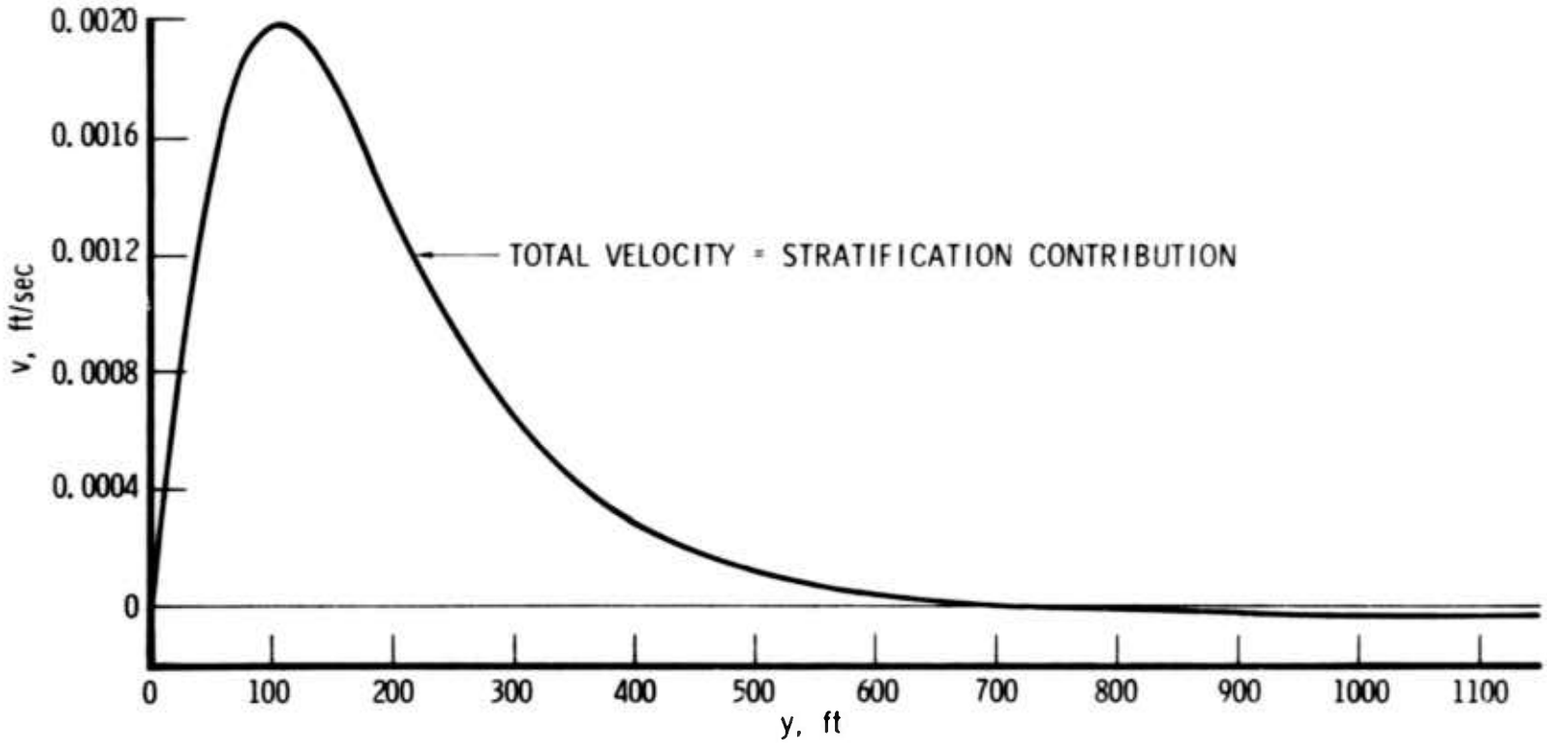

Fig. 14. y-Component of Surface Velocity in x=0 Plane (Body in Thermocline)

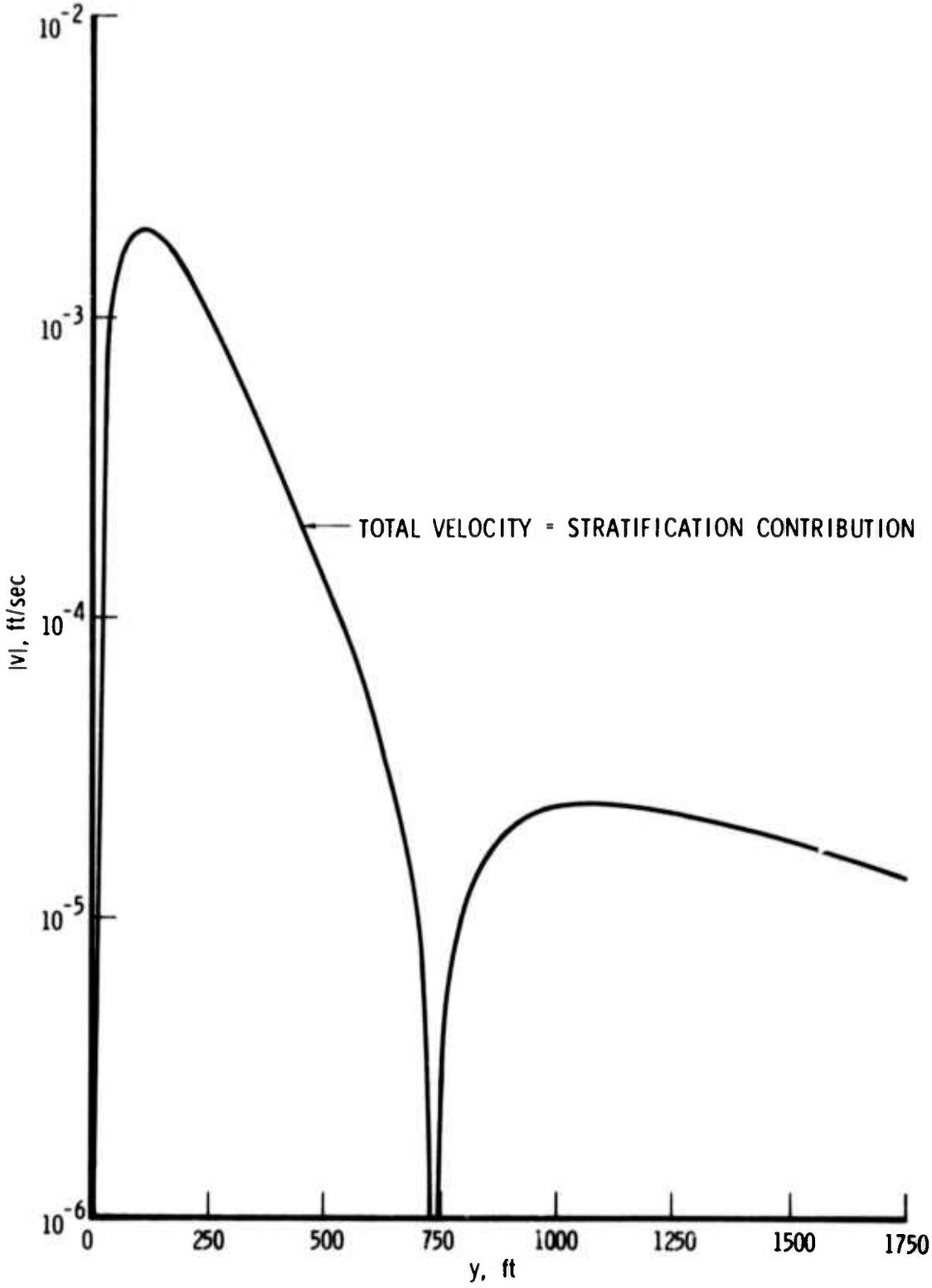

Fig. 15. y-Component of Surface Velocity in x=0 Plane (Body in Thermocline)

VI. CONCLUSIONS

The near-field disturbance created by a slender body in a stratified fluid has been investigated. This problem was made tractable by showing that the governing equations admit a singular perturbation expansion with one expansion valid near the body and one far downstream of the body. The near-field equations resulting from this expansion are substantially simpler than previously published equations and are solved analytically. The far-field equations are also derived for completeness and are found to be simpler than the more general set. Previous investigations of this problem have assumed that the free surface is a plane; the perturbation equations which result from relaxing this assumption are derived and solved analytically.

An immediate new result arising from the analytic solution is the appearance of a singularity on the axis behind the body. The reasons for the existence of the singularity and techniques for removing it are discussed. It is ultimately concluded that the singularity has little impact on the predicted values of surface disturbance. However, a knowledge of the existence of this singularity may be important when flows of this type are calculated using numerical schemes, which cannot treat singularities without special provisions.

Typical calculations have been made using the analytic solutions, and these results are presented in graphical form. The disturbance at the surface is broken down into three components: zero order potential flow, stratification contribution, and gravity wave contribution. For the particular cases considered, the dominant surface disturbance is generated by the zero order potential flow, with significant corrections being made by the stratification effect. For bodies at such depths as 150 ft the gravity wave effect is completely negligible; thus, the usual assumption of a plane free surface is justified.

REFERENCES

1. Miles, J. W., "Internal Waves Generated by a Horizontally Moving Source," Geophysical Fluid Dynamics, 2, 1971, pp. 63-87.

2. Carrier, G. F., and A. Chen, "Internal Waves Produced by Underwater Vehicles," Report 182-6001-RO-00, TRW Systems, Redondo Beach, California, November 1971.

3. Milder, M., "Internal Waves Radiated by a Moving Source," Report 2702-007, R&D Associates, Santa Monica, California, February 1974.

4. Saffman, P. G., "The Motion of a Vortex Pair in a Stratified Atmosphere," Studies in Applied Math, LI(2), June 1972, pp. 107-119.

5. Van Dyke, M., Perturbation Methods in Fluid Mechanics, Academic Press, New York, 1964.

ACRONYMS AND SYMBOLS

d	depth of the body (or source) beneath the free surface
F	internal wave function defined by Eqs. (56) through (61)
g	gravitational acceleration
G	gravity wave function defined by Eq. (42)
i	unit vector
J	Bessel function
k	Vaisala wave number defined by Eq. (16)
ℓ	one-half the separation of the source sink pair creating the disturbance
L	bound of constant thermocline region
m	source-strength constant appearing in the fundamental solution to Laplace's equation
p	pressure
r	radial coordinate measured from the z axis
R	coordinate in Fourier space
S	source solution to Laplace's equation defined in Eq. (33)
u	x component of perturbation velocity [Eq. (6)]
v	cross-track velocity component
$\overline{V}$	vector velocity
w	vertical velocity component
W	internal wave solution function defined by Eq. (45)
x	coordinate parallel to the flow direction
X	rescaled x variable defined in Eq. (26)

y	cross-track coordinate
z	vertical coordinate
∇	symbolic vector differential operator
ζ	z component of vorticity
η	y component of vorticity
Θ	rescaled far-field vorticity function defined in Eq. (30)
ξ	x component of vorticity
ρ	density
ϕ	velocity potential defined in Eq. (13)
Φ	rescaled far-field velocity potential defined in Eq. (29)
χ	dummy variable defined by Eq. (46)
ψ	dummy variable defined by Eq. (35)
Ψ	Hankel transform of ψ
$\vec{\omega}$	vector vorticity
Ω	vorticity function defined by Eq. (14)

Subscripts

G	perturbation associated with gravity wave
I	perturbation associated with internal wave
0	nominal value used as a basis for perturbations; reference value
1	first order perturbation quantity; solution with body in thermocline
2	solution with body outside thermocline
∞	refers to freestream value